

# Carbon nanotubes degraded by neutrophil myeloperoxidase induce less pulmonary inflammation

Valerian E. Kagan,<sup>1,\*</sup> Nagarjun V. Konduru,<sup>1</sup> Weihong Feng,<sup>1</sup> Brett L. Allen,<sup>2</sup>  
Jennifer Conroy,<sup>3</sup> Yuri Volkov,<sup>3</sup> Irina I. Vlasova,<sup>1</sup> Natalia A. Belikova,<sup>1</sup> Naveena  
Yanamala,<sup>4</sup> Alexander Kapralov,<sup>1</sup> Yulia Y. Tyurina,<sup>1</sup> Jingwen Shi,<sup>6</sup> Elena R. Kisin,<sup>7</sup>  
Ashley R. Murray,<sup>7</sup> Jonathan Franks,<sup>5</sup> Donna Stolz,<sup>5</sup> Pingping Gou,<sup>2</sup> Judith Klein-  
Seetharaman,<sup>4</sup> Bengt Fadeel,<sup>6</sup> Alexander Star<sup>2</sup> and Anna Shvedova<sup>7</sup>

<sup>1</sup> Center for Free Radical and Antioxidant Health, Department of Environmental and  
Occupational Health, University of Pittsburgh, Pittsburgh, PA; <sup>2</sup>Department of  
Chemistry, University of Pittsburgh, Pittsburgh, PA;

<sup>3</sup>Department of Clinical Medicine and Centre for Research on Adaptive  
Nanostructures and Nanodevices (CRANN), Trinity College Dublin, Dublin, Ireland;

<sup>4</sup>Department of Structural Biology and <sup>5</sup>Department of Cell Biology and Physiology,  
University of Pittsburgh, Pittsburgh, PA; <sup>6</sup>Division of Molecular Toxicology, Institute of  
Environmental Medicine, Karolinska Institutet, Stockholm, Sweden; <sup>7</sup>Pathology and  
Physiology Research Branch, Health Effects Laboratory Division (HELD), National  
Institute for Occupational Safety and Health (NIOSH) and Department of Physiology and  
Pharmacology, West Virginia University, Morgantown, WV.

**\*Correspondence to:** Prof. Valerian E. Kagan, Center for Free Radical and Antioxidant Health, Department of Environmental and Occupational Health, University of Pittsburgh, Bridgeside Point 100 Technology Drive, Suite 350, Pittsburgh, PA, USA. Tel.: +1 412 624 9479; Fax: +1 412 624 9361; E-mail: [kagan@pitt.edu](mailto:kagan@pitt.edu)

**Running title:** Biodegradation of carbon nanotubes.

**Key words:** single-walled carbon nanotubes; myeloperoxidase; neutrophil; biodegradation; pulmonary inflammation.

## Supporting Information

### Supplementary Figures

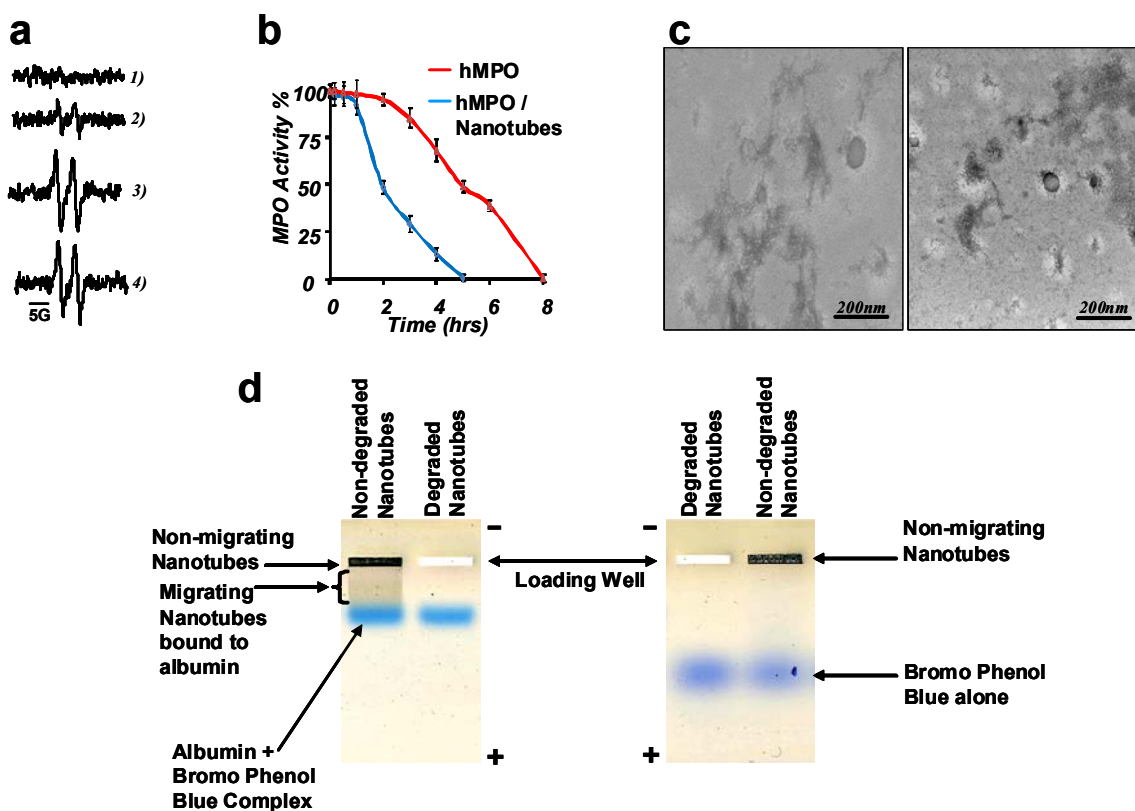


**Figure S1. hMPO peroxidase activity measurements and characterization of biodegraded material.** **a**, EPR spectra of ascorbate radicals characterizing peroxidase activity of hMPO in the presence and absence of nanotubes. 1) nanotubes alone, 2) hMPO and nanotubes, 3) hMPO and  $\text{H}_2\text{O}_2$  and 4) nanotubes, hMPO and  $\text{H}_2\text{O}_2$ . Addition of nanotubes to the incubation mixture did not change the EPR signal of ascorbate radical. In the absence of hMPO or  $\text{H}_2\text{O}_2$ , the magnitude of the signal was several-fold lower thus confirming that oxidation of ascorbate occurred mainly via the peroxidase reaction. **Incubation conditions:** hMPO ( $0.35 \mu\text{M}$ ) was incubated with nanotubes ( $0.02 \text{ mg/ml}$ ) for 1 min at room temperature in phosphate buffer saline (PBS), then ascorbate ( $100 \mu\text{M}$ ) was added and the peroxidase reaction was initiated by  $\text{H}_2\text{O}_2$  ( $80 \mu\text{M}$ ). EPR spectra of ascorbate radicals were recorded 1 min after addition of  $\text{H}_2\text{O}_2$ . EPR spectra were recorded on a JEOL REIX spectrometer with 100 kHz modulation (JEOL, Kyoto, Japan). Measurements were performed at room temperature in gas permeable Teflon tubing ( $0.8 \text{ mm}$  internal diameter,  $0.013 \text{ mm}$  thickness) obtained from Alpha Wire Corporation (Elizabeth, NJ). The tubing was filled with  $60 \mu\text{l}$  of sample, folded doubly, and placed in an open  $3.0 \text{ mm}$  internal diameter EPR quartz tube. EPR spectra of ascorbate radicals were recorded at  $3350 \text{ G}$ , center field;  $50 \text{ G}$ , sweep width;  $10 \text{ mW}$ , microwave power;  $0.5 \text{ G}$ , field modulation;  $10^3$ , receiver gain;  $0.1 \text{ s}$ , time constant;  $1 \text{ min}$ , scan time. **b**, hMPO activity measurements in the presence and absence of nanotubes based on standard guaiacol assay. **Assay conditions:** Guaiacol ( $100 \text{ mM}$  final concentration) was incubated with nanotubes ( $25 \mu\text{g}$ )/hMPO ( $2.5 \mu\text{g/ml}$ ) biodegradation incubation system at  $25^\circ\text{C}$  reinitiated by addition of  $\text{H}_2\text{O}_2$  ( $500 \mu\text{M}$ ) in a total volume of  $1.0 \text{ mL}$ . Absorbance was recorded at  $470 \text{ nm}$  until constant. **c**, TEM images of biodegraded nanotubes showing

fields with globular carbonaceous amorphous material **d**, Agarose gel electrophoresis showing mobility profiles of non-biodegraded and biodegraded material in 0.5 % agarose. Electrophoresis was performed in TAE buffer (40 mM Tris acetate and 1 mM EDTA) and the wells were loaded with 20  $\mu$ L of the material. The majority of the non-biodegraded nanotubes loaded on the native 0.5 % agarose gel (Fig. S1d), - particularly those that were aggregated or bundled - did not enter the gel resulting in the congestion of nanotubes in the loading well. A small fraction of the non-biodegraded nanotubes in the sample migrated towards the anode causing dark smears/streaks on the gel upon co-incubation with albumin/bromophenol blue, likely due to their non-specific binding to the protein. Under similar conditions, non-biodegraded nanotubes loaded onto the wells in the absence of albumin (but in the presence of bromophenol blue alone), did not produce dark smears/streaks (Fig. S1d, right panel). Note that the migration of bromophenol blue in the presence and absence of albumin in native gel was different reflecting the interactions of the dye with the protein (compare the right and the left panels). As indicated in the text (p. 3, para. 2) short-cut nanotubes contain carboxyl groups on their surface and terminal ends (Wei. Z., et al, JACS, 2006; Liu. J et al, Science, 1998). Both the size of the nanotubes and the number of negatively charged groups may vary. These small negatively charged nanotubes non-specifically bound to albumin/bromophenol blue produce the dark smear during native agarose gel electrophoresis. Most importantly, when the biodegraded nanotubes were loaded onto the wells, neither the congested black band nor the dark smear were observed on the native gel. This indicates that biodegradation resulted in disappearance of different types of nanotubes detectable by native agarose electrophoresis. Albumin – with a molecular weight of 64 kDa - was readily detectable by binding with bromophenol blue.

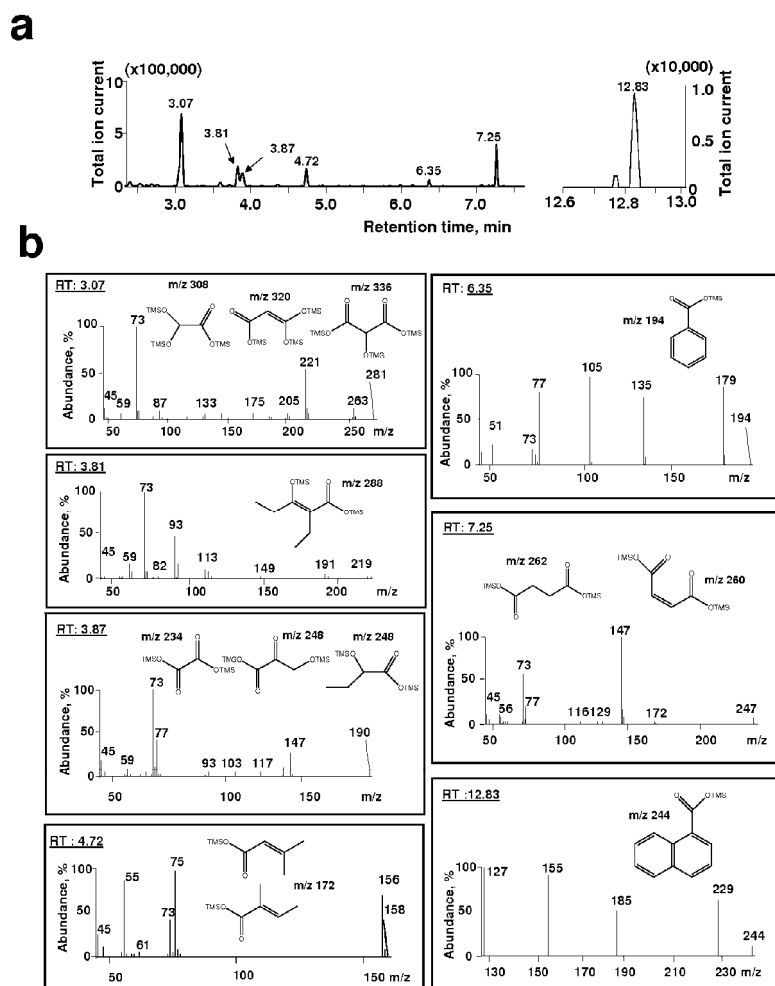


**Figure S2. GC-MS analysis of nanotubes biodegradation products.** **a**, Typical GS-MS chromatogram of products obtained from *partially* degraded nanotubes. **b**, MS-fragmentation patterns of major nanotubes biodegradation products (chemical formulas are presented on the respective panels) corresponding to characteristic peaks with retention times shown on Fig. S2a. The short-chained tri-, di- and mono- carboxylated alkanes and alkenes (retention time 3.07 min, 3.81 min, 3.87 min, 4.72 min, 7.25 min), benzoic acid (retention time 6.35 min) and naphthoic acid (retention time 12.83 min) are shown.

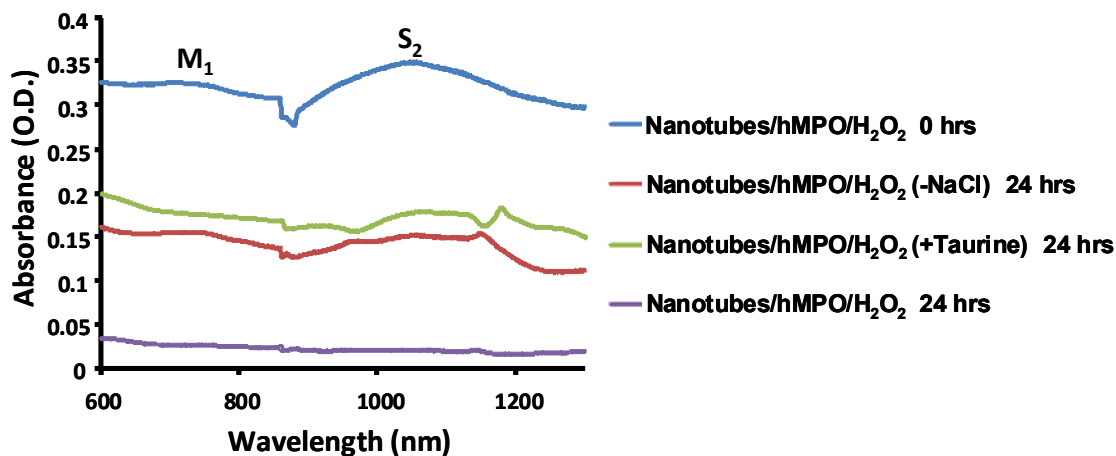


**Figure S3. Effect of taurine on biodegradation of nanotubes.** Vis-NIR spectroscopic evaluation of nanotubes biodegradation when incubated with hMPO/H<sub>2</sub>O<sub>2</sub> in the standard incubation buffer containing 140 mM NaCl either in the presence of 10 mM taurine (green) or when incubated in buffer without NaCl (red).

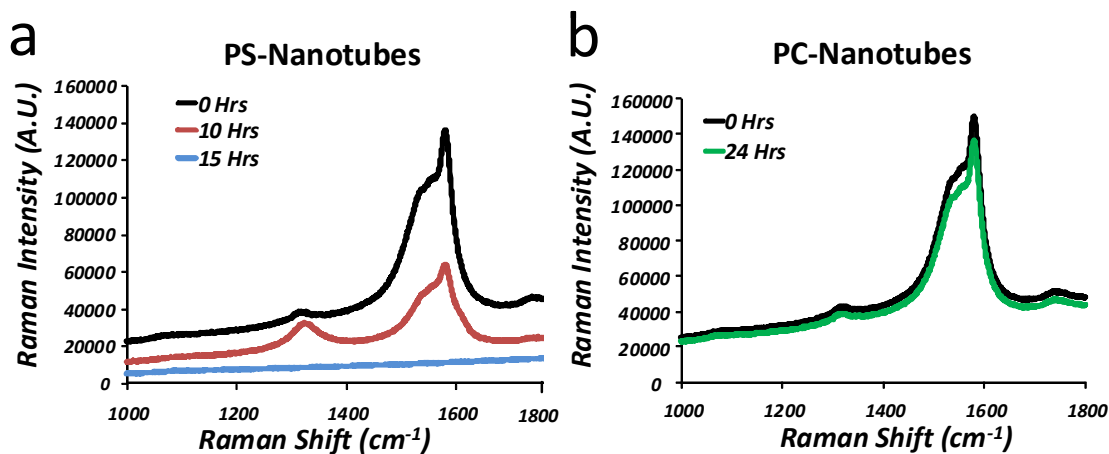


**Figure S4. Biodegradation of nanotubes coated with phospholipids.** Raman spectroscopic analysis of time dependent degradation of (a) PS- and (b) PC-coated nanotubes incubated with hMPO/ $\text{H}_2\text{O}_2$  in 50 mM phosphate buffer containing 140 mM NaCl under standard *in vitro* conditions (see Methods for coating procedure for nanotubes).

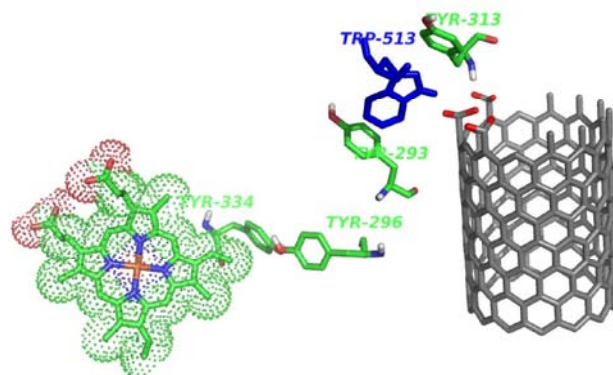


**Figure S5. Proposed model for the mechanism of radical transfer via a network of amino acids bridging the heme site with the nanotubes binding site.** The nanotubes is colored in grey with the exception of oxygen atoms which are colored in red. Tyrosine residues and the heme are colored in CPK colors. Tryptophan is colored in blue. All the residues involved in this network are rendered as sticks and labeled with the respective residue identifier. The heme is rendered in sticks and surface dots.

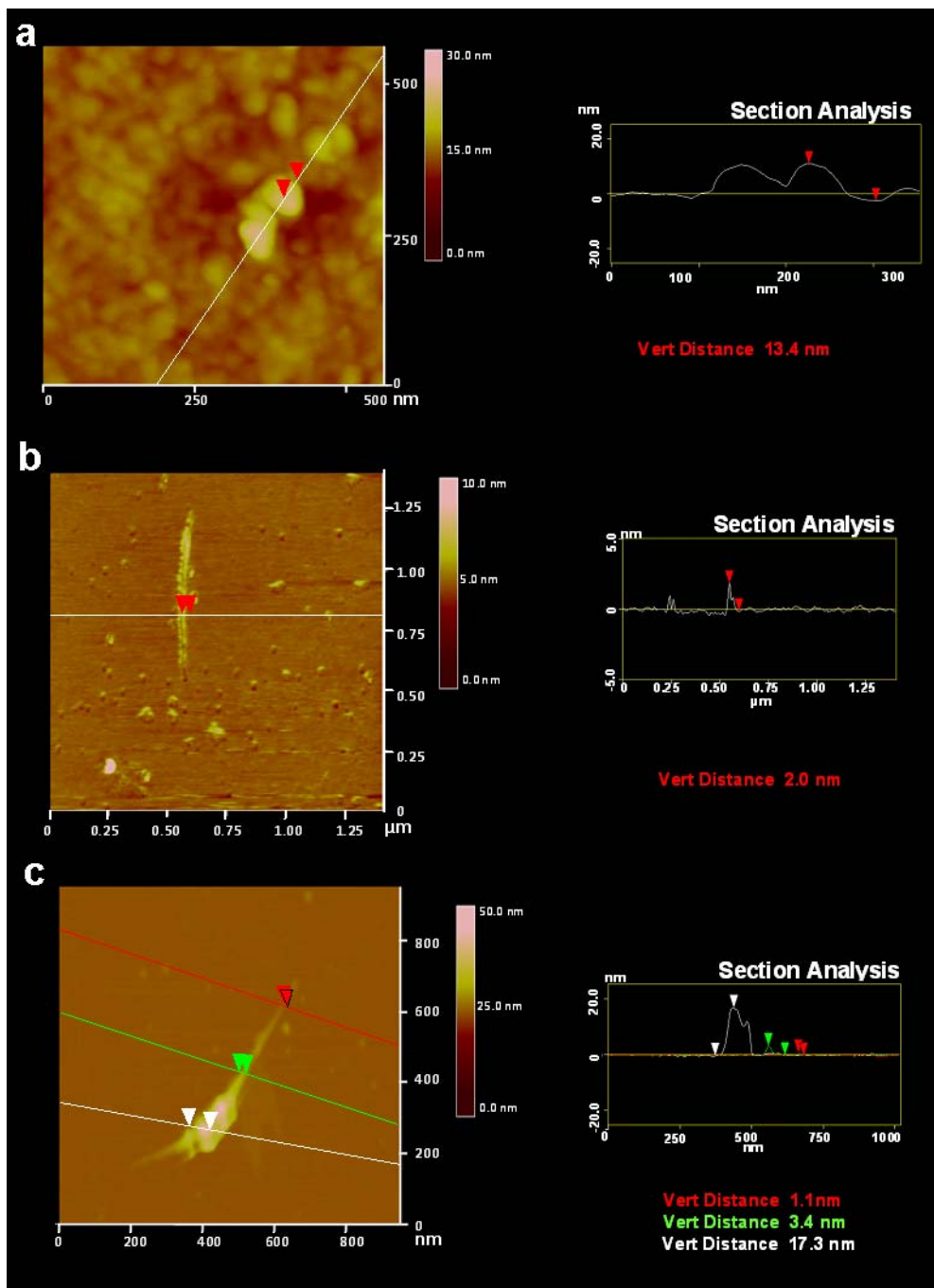


**Figure S6. Section analysis of hMPO incubated with nanotubes using Atomic Force Microscopy (AFM).** Section analysis of **a**, purified hMPO. **b**, bare nanotubes and **c**, hMPO incubated with nanotubes deposited on mica substrates (see Methods section regarding sample preparation and analysis).

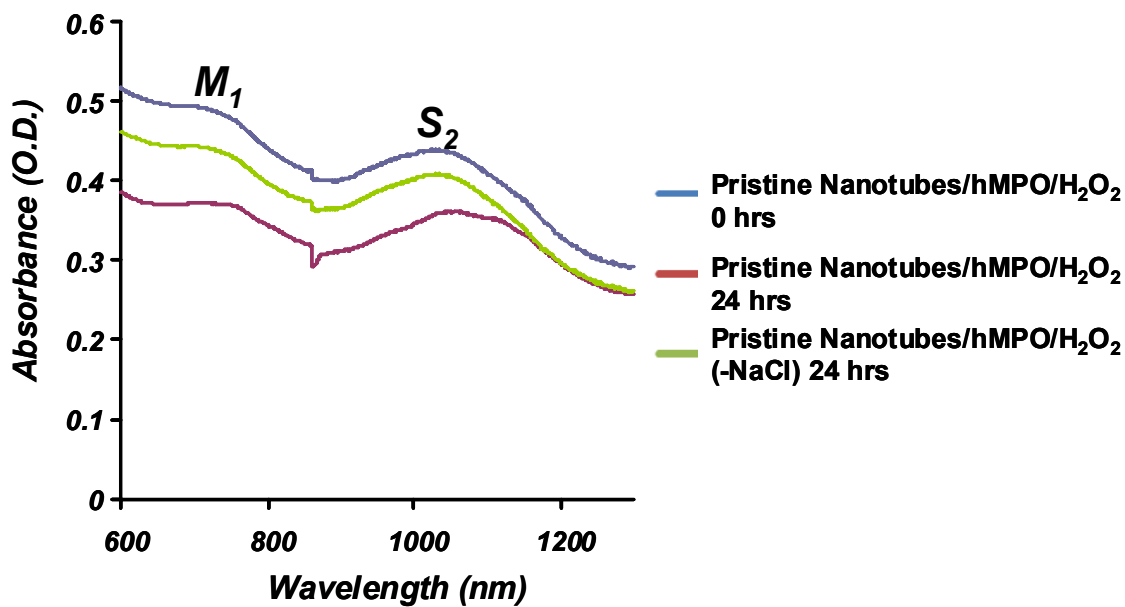


**Figure S7. Biodegradation of pristine nanotubes by hMPO.** Vis-NIR spectroscopic analysis showing pristine nanotubes before (blue line) and after 24 hrs of enzymatic catalysis with hMPO/H<sub>2</sub>O<sub>2</sub> in 50 mM phosphate buffer, without (green line) and with (red line) 140 mM NaCl.

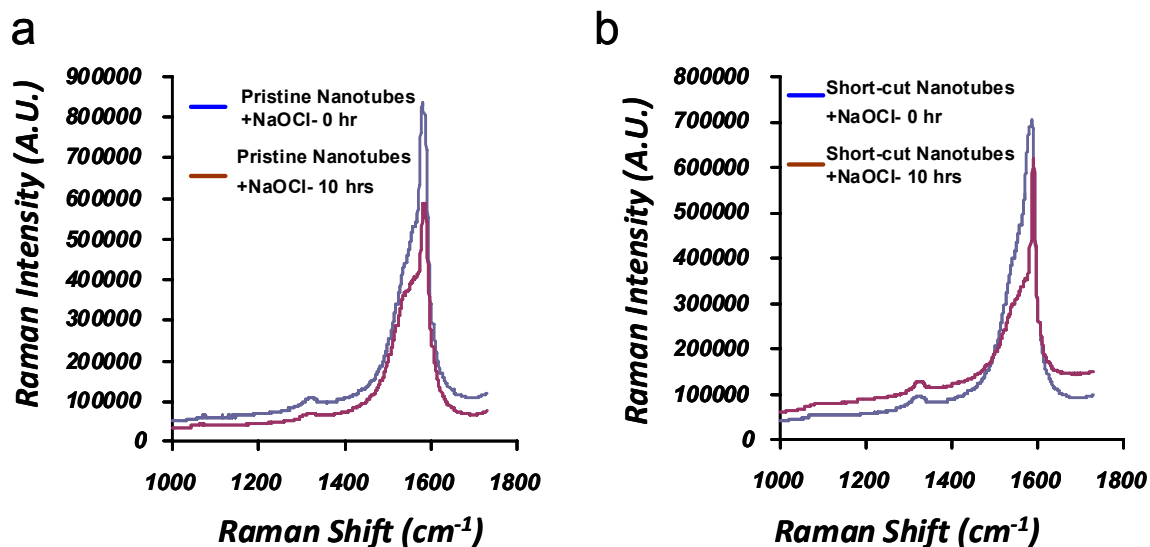


**Figure S8. Raman spectroscopic analysis of pristine nanotubes and short-cut nanotubes incubated with sodium hypochlorite (NaOCl).** Analysis showing effects of hypochlorite on (a) Pristine nanotubes and (b) short-cut nanotubes after 10 hrs of incubation. Sodium hypochlorite (200  $\mu\text{M}$  final) was added every hour for 10 hrs to the carbon nanotube particles incubated in 50 mM phosphate standard incubation buffer at 37°C.

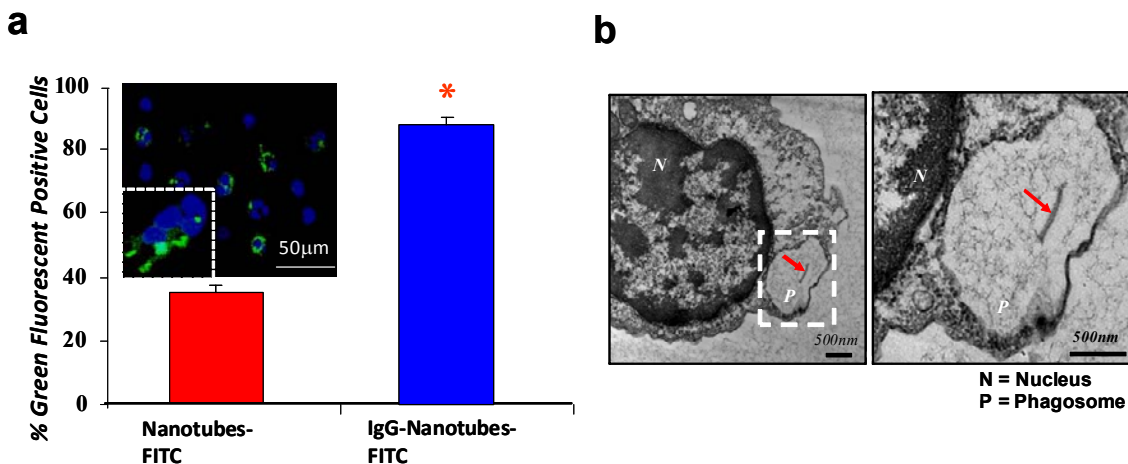


**Figure S9. Uptake of nanotubes conjugated with fluorescein isothiocyanate (FITC) (nanotubes-FITC) and functionalized with IgG by human peripheral blood neutrophils.** **a**, Quantitative assessment of nanotubes-FITC uptake by neutrophils isolated from human blood after co-incubation for 2 hrs at 37°C. A total of 500 cells from each sample type were analyzed by fluorescence microscopy. Data are mean values ± S.D. (n = 3, \*p<0.05). **Insert**, Confocal micrograph of neutrophils following incubation with IgG-functionalized nanotubes-FITC for 2 hrs. Blue: cell nuclei, Green: nanotubes-FITC. (Note: The insert also shows a magnified image of a neutrophil with internalized IgG-nanotubes-FITC). **b**, Transmission electron micrograph of a neutrophil phagocytosing IgG-nanotubes. A higher magnification view of the neutrophil phagosome with IgG-nanotubes is also shown. (Arrows point to IgG-nanotubes).

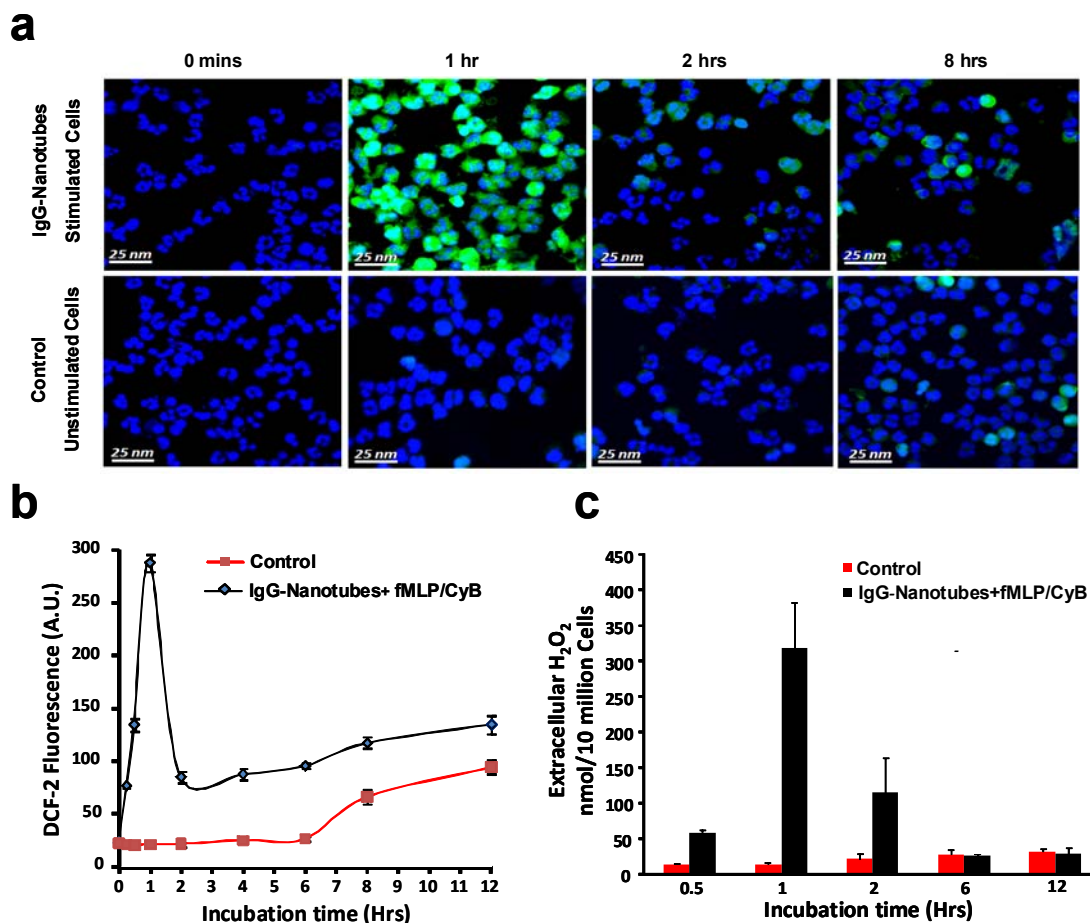


**Figure S10. Generation of H<sub>2</sub>O<sub>2</sub> in stimulated neutrophils.** **a**, micrographs exhibiting 2,7-dichlorofluorescein (DCF) fluorescence (as a measure of intracellular H<sub>2</sub>O<sub>2</sub>) of intracellular H<sub>2</sub>O<sub>2</sub> production in human neutrophils at different time points. DCF fluorescence was captured using laser confocal scanning microscope (excitation at 488 nm). Blue: cell nuclei, Green: DCF fluorescence. **b**, Time-course of mean DCF fluorescence (as a measure of intracellular H<sub>2</sub>O<sub>2</sub>) using MetaMorph software (Universal imaging). Data points represent mean fluorescence values  $\pm$  S.D. of 200 cells from 3 determinations, and **c**, measurements of extra-cellular H<sub>2</sub>O<sub>2</sub> from neutrophils stimulated with fMLP/cyB and incubated with IgG-nanotubes using Amplex red.

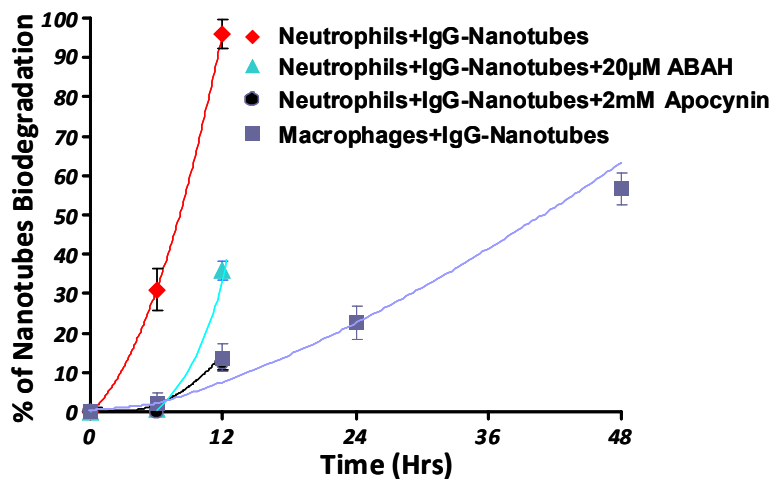


**Figure S11. Biodegradation of IgG-nanotubes by neutrophils and macrophages.**

Cells ( $25 \times 10^6$ ) were incubated with  $25 \mu\text{g}$  of IgG-nanotubes for 12-48 hrs (12 hrs for Neutrophils and up-to 48 hrs for macrophages) and the extent of biodegradation was assessed. Neutrophils were pre-treated with either  $20 \mu\text{M}$  4-aminobenzoic acid hydrazide (ABAH) or  $2 \text{mM}$  apocynin for 1 hr prior to the addition of IgG-nanotubes. The level of biodegradation at different time points is plotted as percentage ( $n=3$ ) assessed by the intensity magnitudes of both the characteristic semi-conducting ( $S_2$ ) and the metallic ( $M_1$ ) peaks of nanotubes present in the recorded Vis-NIR spectra.

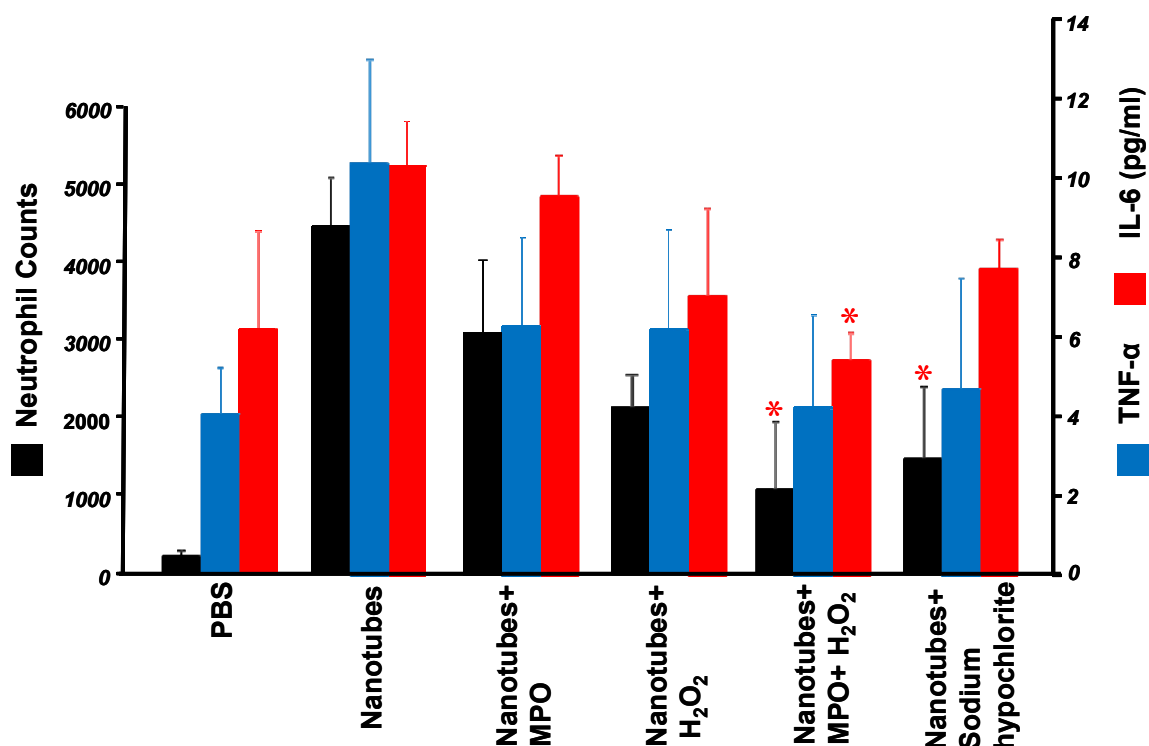


**Figure S12. Pro-inflammatory pulmonary response in C57BL/6 mice to nanotubes and biodegraded nanotubes.** Neutrophil counts and expression of TNF- $\alpha$  and IL-6 in bronchoalveolar lavage fluid were measured 7 days after exposure to the indicated treatments via the pharyngeal aspiration. Data shown represent means values  $\pm$  S.E. ( $n = 6$  mice per group). \* $p < 0.05$  vs. nanotubes alone. Biodegradation of nanotubes was induced by their incubation with hMPO/H<sub>2</sub>O<sub>2</sub> system.

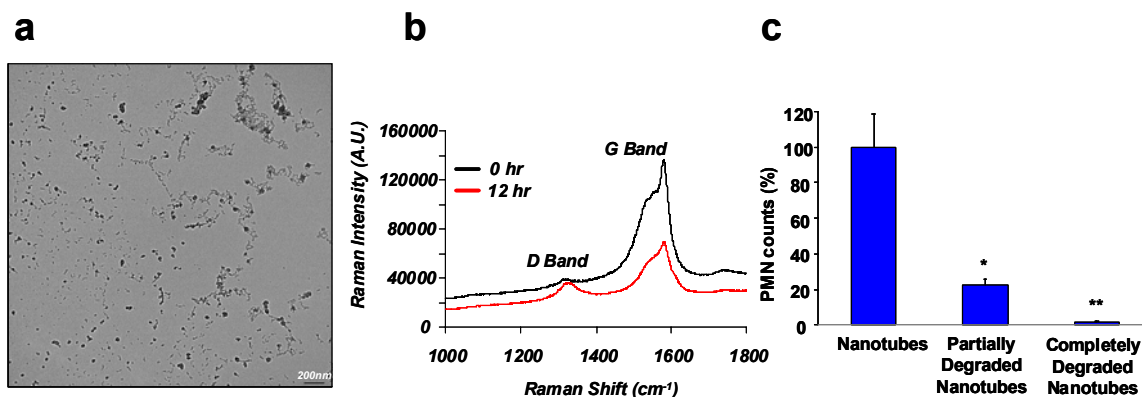


**Figure S13. Electron microscopic and Raman spectroscopic analysis of partially biodegraded (12 hrs incubation with hMPO/H<sub>2</sub>O<sub>2</sub>) nanotubes and their effects on neutrophil response after pharyngeal aspiration in C57BL/6 mice.**

**a**, shows transmission electron micrograph of partially degraded nanotubes. The sample was prepared from an aliquot corresponding to 12 hrs incubation of nanotubes with hMPO/H<sub>2</sub>O<sub>2</sub>. **b**, Raman spectra showing lowering of G-band and an increase in the D-band in the partially degraded nanotubes (red line) compared to the untreated or non-degraded nanotubes (black line). **c**, Shows neutrophil counts from pharyngeal aspiration of nanotubes in BAL fluid from the exposed mice. Data are mean values ± S.D., n=6. \**p*<0.01, partially degraded nanotubes vs nanotubes; \*\**p*<0.001, completely degraded nanotubes vs nanotubes. (**Note:** Non-degraded implies to material not treated with hMPO/H<sub>2</sub>O<sub>2</sub> and completely degraded nanotubes corresponds to the material from hMPO/H<sub>2</sub>O<sub>2</sub>/nanotubes incubation system at 24 hrs showing complete loss in the characteristic spectral and morphological features as presented in Fig. 1)

## Supplementary Tables:

**Supplementary Table S1.** Comparison of the results of computational docking pristine and carboxylated nanotubes to hMPO. The 5Å binding pocket residues along with the binding site location, interaction energies and number of conformations observed in each binding site are listed for both pristine and carboxylated nanotubes. The final intermolecular energy (van der Waals + hydrogen bond + desolvation energy + electrostatic energy) and the binding energy (intermolecular energy + total internal energy + torsional free energy – unbound system energy) are also listed for the two predicted binding sites. The residues that are unique to the two binding sites are highlighted in bold and colored in blue and red for the first and second binding site, respectively. The tyrosine and arginine residues of the first binding site that involves the catalytically active residues (colored in red and yellow in main manuscript Figure 2, B and C) are highlighted in bold.

	<i>Binding site location</i>	<i>Binding Energy (# of conformations)</i>	<i>Final Intermolecular Interaction energy</i>	<i>5Å Residues</i>
<i>Pristine (14,0)</i>	<i>At the catalytically active site (first binding site)</i>	<i>-16.53 (23/25)</i>	<i>-16.53</i>	<i>Tyr293, Arg294, Asp295, Pro298, Leu299, Pro303, Met306, Arg307, Leu310, Pro311, Thr312, Tyr313, Lys488, Arg507, Glu515, Asn549, Asn550, Met553</i>
	<i>At the distal end of heme group (second binding site)</i>	<i>-12.74 (2/25)</i>	<i>-12.74</i>	<i>Asn26, Phe99, Pro101, Glu102, Pro103, Ala104, Ile164, Ala166, Glu180, Pro182, Leu183, His217, Thr238</i>
<i>Carboxylated nanotubes (14,0)</i>	<i>At the catalytically active site (first binding site)</i>	<i>-15.7 (16/25)</i>	<i>-17.16</i>	<i>Tyr293, Arg294, Asp295, Pro298, Leu299, Pro303, Met306, Arg307, Leu310, Pro311, Thr312, Tyr313, Lys488, Arg507, Trp513, Trp514, Glu515, Asn549, Asn550, Met553</i>
	<i>At the distal end of heme group (Second binding site)</i>	<i>-11.20 (9/25)</i>	<i>-12.65</i>	<i>Asn26, Phe99, Pro101, Glu102, Pro103, Ala104, Pro154, Ile164, Ala166, Glu180, Pro182, Leu183</i>

### **Supplementary Materials and Methods:**

**Reagents:** HEPES, MgCl<sub>2</sub>, KCl, NaCl, phenylmethylsulfonyl fluoride, paraformaldehyde, glutaraldehyde, guaiacol, osmium tetroxide, potassium ferricyanide, diethylenetriaminepentaacetic acid (DTPA), N, N-dimethylformamide (DMF), N-formyl-met-leu-phe (fMLP), hydrogen peroxide, hypochloric acid, and Hoechst 33342 were from Sigma-Aldrich (St. Louis, MO, USA). RPMI, Ca<sup>2+</sup> + Mg<sup>2+</sup>-free PBS were purchased from Invitrogen Corporation (Grand Island, NY, USA).

**Chemical cleavage of nanotubes:** The procedure was performed as reported previously<sup>1</sup>. Purified nanotubes were dispersed in 4:1 mixture of concentrated H<sub>2</sub>SO<sub>4</sub> and 35 % aqueous (aq) H<sub>2</sub>O<sub>2</sub> and sonicated in ultrasonic bath (Branson 1510 Sonifier®, output power of 70 W at 40 KHz) for 24 hrs at 0 °C. The dispersion was then heated to 70 °C for 10 min for “polishing” the nanotubes. This solution was then diluted 10-fold by deionized water and filtered through PTFE membrane (100 μm pore size). The collected sample was thoroughly washed with deionized water and vacuum dried at 110°C for 30 min. Thus obtained short nanotubes were dispersed in 25 mM HEPES buffer (pH 7.4; containing 150 mM NaCl) by sonication to final concentration 0.5 mg Nanotubes/ml.

**Transmission electron microscopy:** A FEI-Morgani TEM instrument (Tokyo, Japan) was operated at 80 KV equipped with a soft imaging system charge-coupled device (CCD) camera. TEM samples were prepared by drop casting the solution on a copper grid and the excess drawn off with filter paper. Alternatively, one drop of the

aliquot was then placed on a lacey carbon grid (Pacific-Grid Tech, CA, USA) and allowed to dry in ambient conditions for 2 hrs prior to TEM imaging (FEI Morgagni, 80 keV).

***Dynamic light scattering analysis:*** A Malvern Zetasizer Nano (Malvern Instruments, Westborough, MA, USA) was used. The analysis was conducted according to standard operating procedures as previously described<sup>2</sup>. Particle sizes were determined on the basis of the refractive index of carbon as the particle and DMF as the carrier fluid.

***Atomic force microscopy (AFM):*** A multimode scanning probe microscope was utilized in a tapping mode for height, phase, and sectional analysis. Sample preparation was performed on freshly cleaved mica treated with approximately 20  $\mu\text{L}$  of 0.01% (w/w) Poly – L- Lysine (aq) through spin-coating at 1,400 r.p.m. Approximately 10  $\mu\text{L}$  of sample (aq) was spin-coated at 1,400 r.p.m. and allowed to dry in ambient conditions for 45 mins prior to imaging. For non-aqueous samples, treatment of mica with poly – L – Lysine was omitted. Using a “Supersharpe” Si probe (tip radius  $<5$  nm, AppNano), tapping mode was employed at a drive frequency of 182.316 Hz, an amplitude set point of 0.2465 V, and a drive amplitude of 216 mV was performed. Images were initially scanned in a 13.1  $\mu\text{m}$  area prior to magnification of relevant areas. Post imaging processing included sectional analysis for quantifying cross-sectional heights of samples.

***AFM imaging of hMPO/nanotubes interaction*** was performed on freshly cleaved mica treated with Poly – L- Lysine. Approximately 10  $\mu\text{L}$  from the sample (aq) containing nanotubes and hMPO incubated for an hour in 50 mM phosphate buffer was

spin-coated at 1,400 r.p.m. and allowed to dry in ambient air for 45 mins prior to imaging.

***Gel-electrophoresis:*** Electrophoresis for assessing mobility profiles of non-biodegraded and biodegraded nanotubes was carried out in a 0.5% agarose gel that can act as a sieve for the carbon nanotubes as they migrate in an electric field. Electrophoresis was performed in TAE buffer (40 mM Tris acetate and 1 mM EDTA) and the wells were loaded with 20  $\mu\text{L}$  of the nanotubes suspension (corresponding to 10  $\mu\text{g}/\mu\text{L}$  in the control samples).

***Raman spectroscopy:*** Samples suspended in ethanol were prepared by drop-casting approximately 20  $\mu\text{L}$  on a quartz microscope slide and allowed to dry. A Renishaw inVia Raman microscope spectrometer (Renishaw, Gloucestershire, UK) with an excitation wavelength of 633 nm was used for all samples, while scanning 1000 – 1800  $\text{cm}^{-1}$  to visualize D and G band intensity changes throughout the degradation process. Spectra were collected with a 15 second exposure time and averaged across 5 scans per sample.

***Gas chromatography-mass spectroscopy (GC-MS) of  $\text{CO}_2$ :*** Approximately 2  $\mu\text{L}$  of sample headspace from a typical incubation medium containing nanotubes plus hMPO and  $\text{H}_2\text{O}_2$  was injected into a Shimadzu QP5050A GC-MS unit (Shimadzu Instruments, Columbia, MD, USA) with an XTI-F capillary column (30 m, 0.25 mm i.d., 0.25  $\mu\text{m}$  film thickness). A basic temperature program was run starting at 100  $^\circ\text{C}$  held for one minute,

followed by temperature ramping at a rate of 10 °C/min until a maximum of 325 °C was achieved and held for an additional 10 min. CO<sub>2</sub> (with m/z 44) intensities were observed relative to N<sub>2</sub> (28 m/z) and analyzed for their maximum concentration.

***Determination of nanotubes biodegradation products by GS-MS:*** The biodegradation products of nanotubes were extracted from incubation media and detected using GS-MS as described by Zeinali et al.<sup>3</sup> and Meckenstock et al.<sup>4</sup>. Incubation medium without nanotubes was used as a control sample. Briefly, biodegraded nanotubes products were extracted twice with three volumes of ethyl acetate. The extracts were evaporated under nitrogen, dissolved in hexane:ethyl acetate (99:1 v/v) and derivatized with reagent (99% N,O-bis(trimethylsilyl)-trifluoroacetamide (BSTFA)+1% trimethylchlorosilane (TMCS)) at 60 °C for 40 min. The GC-MS analysis was performed on GC-2010 gas chromatograph (Shimadzu, Japan) equipped with a DB-225MS capillary GC column (30 m, 0.25 mm i.d., 0.25 µm film thickness, Agilent Technologies, Santa Clara, CA) and coupled to a GCMS-QP2010S mass spectrometer. GC temperature program was 280 °C interface temperature, 100 °C (2 min isothermal), 100-250 °C (at 10 °C/min) and 250 °C (3 min isothermal). Helium was used as a carrier gas at a flow rate of 0.97 ml/min. GS-MS conditions: positive electron ionization (EI+); ionization electron energy, 70 eV; source temperature, 200 °C and mass range m/z 45-800. The mass spectra of individual total ion peaks were identified by comparison with mass spectra database (Shimadzu, Japan).

**Coating of SWCNT with phospholipids:** Coating of nanotubes with PS or PC was performed essentially as described previously<sup>2</sup>. SWCNT were sonicated with either 2.5 mM DOPC or 5 mM DOPC:DOPS at the ratio of 1:1 (3 cycles 30 secs), then washed 4 times with 25 mM HEPES, pH 7.4. After each washing, samples were centrifuged at 50,000 g for 30 min at 4°C. Coated SWCNT were finally suspended in 25 mM HEPES pH 7.4 (containing a transition metal chelator, DTPA (100 µM) to prevent oxidative damage to lipids) using the same volume as the original suspension.

**Neutrophils isolation:** Human neutrophils were isolated by a procedure utilizing Histopaque (Sigma, St. Louis, MO, USA). Briefly, human buffy coat (Central blood bank, Greentree, PA, USA) was layered on top of a density gradient (Histopaque1.077/1.119, Sigma, St. Louis, MO, USA) and subjected to centrifugation as described in the manual (700 g 45 min at room temperature without brake). The neutrophil-rich supernatant (between the layers of Histopaque) was carefully aspirated and washed twice with calcium and magnesium free PBS; thus obtained cells were suspended in RPMI and adjusted to  $25 \times 10^6$  cells/ 3ml before use.

**Isolation of monocyte-derived macrophages** was performed essentially as described.<sup>5</sup> In brief, mononuclear cells were prepared from buffy coats obtained from healthy adult blood donors by density gradient centrifugation using Histopaque1.077/1.119. Cells were washed and resuspended in RPMI-1640 medium. Monocytes were separated by adhesion to tissue culture plastic for 1 hr at 37°C with a 5 % CO<sub>2</sub> atmosphere and non-adherent cells were removed by several washes with PBS.

Human monocyte-derived macrophages were cultured for 3-4 days in RPMI-1640 medium supplemented with 10% heat-inactivated fetal bovine serum, 2 mM glutamine, 100 U/ml penicillin and 100 µg/ml streptomycin (Gibco Invitrogen Corporation, Paisley, UK), and 50 ng/ml human recombinant M-CSF (R&D Systems, Abingdon, UK) prior to assessment of biodegradation.

***Nanotubes labeling by FITC:*** Fluorescent labeling of nanotubes was achieved using commercial single-walled carbon nanotubes (arc discharge, Carbon Solutions, CA, USA) which were chemically cut by H<sub>2</sub>SO<sub>4</sub>/H<sub>2</sub>O<sub>2</sub> as described above and were functionalized with FITC according to the published procedure.<sup>6</sup>

***Uptake of nanotubes by neutrophils:*** All uptake assays were performed in cell culture medium without serum. After incubation with FITC-Nanotubes (25 µg/10<sup>6</sup> cells), neutrophils were washed twice with PBS and fixed using 2.5 % paraformaldehyde. Nuclei were stained with Hoechst 33342. Cells were imaged using an Olympus Fluoview 1000 confocal microscope (Malvern, NY, USA).

***Superoxide generation:*** Oxidation-dependent fluorogenic dye, dihydroethidium (DHE, Molecular Probes, Eugene, OR, USA) was used to evaluate intracellular production of superoxide radicals. Briefly, 0.3 x 10<sup>6</sup> cells were incubated with 5 µM DHE for 10 min prior to treatments. After washing with PBS, cells were incubated with IgG-nanotubes or nanotubes (25 µg) for 30 min. fMLP (10 nM) was used as a control to

trigger ROS generation in cells. Subsequently, treated cells were either collected or fixed for fluorescence microscopy. Cells were examined under a Nikon ECLIPSE TE 200 fluorescence microscope (Tokyo, Japan) equipped with a digital Hamamatsu charge-coupled device camera (C4742-95-12NBR). Extracellular superoxide generated by neutrophils was measured in incubation medium by an SOD-inhibitable cytochrome *c* reduction assay as described by Pick and Mizel (1981)<sup>7</sup>.

**Hydrogen peroxide generation:** Amplex Red assay was applied for assessments of hydrogen peroxide production in neutrophils as described previously<sup>8</sup>. Cells ( $3.6 \times 10^6$ /mL) were incubated with either fMLP or nanotubes together with 50  $\mu$ M Amplex Red (Molecular Probes, CA, USA) and horseradish peroxidase 0.1 U/mL at 37 °C for 30 min followed by centrifugation to remove the pellet. Fluorescence of resorufin (Amplex Red oxidation product) was measured at 590 nm using a spectrofluorometer (RF-5301-PC, Shimadzu, Japan). The 2',7'-dichlorofluorescein diacetate (DCF-2DA) assay for intracellular H<sub>2</sub>O<sub>2</sub> detection was performed by incubating  $2.5 \times 10^6$  cells with 20  $\mu$ M DCF-2DA 30 min prior to the initial addition of stimulants for experiments lasting 2 hr. For experiments lasting longer time, the DCF-2DA was added 30 min prior to the cell harvest. Cells were washed twice with PBS, fixed using 2.5 % paraformaldehyde and cytospinned on glass slide for imaging.

**Animals:** Specific-pathogen-free adult female C57BL/6 mice (7-8 wk) were supplied by Jackson Laboratories (Bar Harbor, ME, USA) and weighed  $20.3 \pm 0.2$  g at time of use. Animals were individually housed in Association for Assessment and

Accreditation of Laboratory Animal Care (AAALAC) approved animal facilities in microisolator cages for one week prior to use. Autoclaved Beta Chip bedding (Northeastern Products Corp., Warrensburg, NY, USA) was changed weekly. Animals were supplied with water and Harlan Teklad, 7913, NIH-31 Modified Mouse/Rat Diet, Irradiated (Harlan Teklad, Madison, WI, USA) and housed under controlled light, temperature and humidity conditions. Experiments were conducted under a protocol approved by the Animal Care and Use Committee of the NIOSH. Mice were randomized into two experimental groups treated with non-degraded nanotubes (nanotubes; nanotubes/H<sub>2</sub>O<sub>2</sub>; and nanotubes/MPO) and degraded nanotubes (Nanotubes/MPO/H<sub>2</sub>O<sub>2</sub> and Nanotubes/Sodium hypochlorite) on day 0. Animals were sacrificed on day 1 or day 7 following exposures.

***Bronchoalveolar lavage (BAL):*** Mice were weighed and euthanized with intraperitoneal injection of sodium pentobarbital (SPB, Fort Dodge Animal Health, Fort Dodge, IA, USA) (>100 mg/kg). The trachea was cannulated with a blunted 22 gauge needle, and BAL was performed using cold sterile Ca<sup>2+</sup> + Mg<sup>2+</sup>-free PBS at a volume of 0.9 ml for first lavage (kept separate) and 1.0 ml for subsequent lavages. Approximately 5 ml of BAL fluid per mouse was collected and pooled in sterile centrifuge tubes. Pooled BAL cells were washed in Ca<sup>+2</sup>+Mg<sup>+2</sup>-free PBS by alternate centrifugation (800 × g for 10 min at 4 °C) and resuspension.

**Statistics:** The results are presented as means  $\pm$  S.D. values from at least three experiments, and statistical analyses were performed by one-way ANOVA. The statistical significance of differences was set at  $p < 0.05$ .

1. Wei, Z., Kondratenko, M., Dao, L.H. & Perepichka, D.F. Rectifying diodes from asymmetrically functionalized single-wall carbon nanotubes. *J. Am. Chem. Soc.* **128**, 3134-5 (2006).
2. Konduru, N.V. et al. Phosphatidylserine targets single-walled carbon nanotubes to professional phagocytes in vitro and in vivo. *PLoS One* **4**, e4398 (2009).
3. Zeinali, M., Vossoughi, M. & Ardestani, S.K. Degradation of phenanthrene and anthracene by *Nocardia otitidiscaviarum* strain TSH1, a moderately thermophilic bacterium. *J. Appl. Microbiol.* **105**, 398-406 (2008).
4. Meckenstock, R.U., Annweiler, E., Michaelis, W., Richnow, H.H. & Schink, B. Anaerobic naphthalene degradation by a sulfate-reducing enrichment culture. *Appl. Environ. Microbiol.* **66**, 2743-7 (2000).
5. Boynton, E.L. et al. The effect of polyethylene particle chemistry on human monocyte-macrophage function in vitro. *J. Biomed. Mater. Res.* **52**, 239-45 (2000).
6. Wu, W. et al. Targeted delivery of amphotericin B to cells by using functionalized carbon nanotubes. *Angew. Chem. Int. Ed. Engl.* **44**, 6358-62 (2005).
7. Pick, E. & Mizel, D. Rapid microassays for the measurement of superoxide and hydrogen peroxide production by macrophages in culture using an automatic enzyme immunoassay reader. *J. Immunol. Methods.* **46**, 211-26 (1981).
8. Lekstrom-Himes, J.A., Kuhns, D.B., Alvord, W.G. & Gallin, J.I. Inhibition of human neutrophil IL-8 production by hydrogen peroxide and dysregulation in chronic granulomatous disease. *J. Immunol.* **174**, 411-7 (2005).